Scientific Research Publishing

Open Journal of Forestry, 2024, 14, 1-18
https://www.scirp.org/journal/ojf
ISSN Online: 2163-0437
ISSN Print: 2163-0429

Geospatial Analysis of Urban Heat Island Effects and Tree Equity

Jillian Gorrell, Sharon R. Jean-Philippe*, Paul D. Ries, Jennifer K. Richards, Neelam C. Poudyal, Rochelle Butler

School of Natural Resources, University of Tennessee, 203 Third Creek Building, Knoxville, Tennessee, USA
Email: *jeanphil@utk.edu

How to cite this paper: Gorrell, J., Jean-Philippe, S. R., Ries, P. D., Richards, J. K., Poudyal, N. C., & Butler, R. (2024). Geospatial Analysis of Urban Heat Island Effects and Tree Equity. *Open Journal of Forestry, 14,* 1-18.
https://doi.org/10.4236/ojf.2024.141001

Received: October 21, 2023
Accepted: November 27, 2023
Published: November 30, 2023

Abstract

In recent decades, Urban Heat Island Effects have become more pronounced and more widely examined. Despite great technological advances, our current societies still experience great spatial disparity in urban forest access. Urban Heat Island Effects are measurable phenomenon that are being experienced by the world's most urbanized areas, including increased summer high temperatures and lower evapotranspiration from having impervious surfaces instead of vegetation and trees. Tree canopy cover is our natural mitigation tool that absorbs sunlight for photosynthesis, protects humans from incoming radiation, and releases cooling moisture into the air. Unfortunately, urban areas typically have low levels of vegetation. Vulnerable urban communities are lower-income areas of inner cities with less access to heat protection like air conditioners. This study uses mean evapotranspiration levels to assess the variability of urban heat island effects across the state of Tennessee. Results show that increased developed land surface cover in Tennessee creates measurable changes in atmospheric evapotranspiration. As a result, the mean evapotranspiration levels in areas with less tree vegetation are significantly lower than the surrounding forested areas. Central areas of urban cities in Tennessee had lower mean evapotranspiration recordings than surrounding areas with less development. This work demonstrates the need for increased tree canopy coverage.

Keywords

Spatial Analysis, Land Cover, Urban Heat Island Effect (UHIE), Evapotranspiration, Tree Canopy, Impervious Surface, GIS Prediction Model, GIS Machine Learning

1. Introduction

1.1. Urban Heat Island Effect

The urban heat island effect (UHIE), first identified in the early 1800s and named by Albert Peppler in 1929, is caused by an increase in impervious surfaces from urbanization, making cities significantly warmer than rural or natural areas. Five factors that contribute to the UHIE are: increased anthropogenic heat (generated by humans or human made items such as buildings, cars, industrial processes), reduced evaporation, increased heat storage, increased net radiation, and reduced convection (Gartland, 2012). Urban heat islands contribute to higher daytime temperatures, reduced nighttime cooling, and higher air-pollution levels. These, in turn, contribute to heat-related deaths and heat-related illnesses such as general discomfort, respiratory difficulties, heat cramps, heat exhaustion, and non-fatal heat stroke (Iungman et al., 2023). Vulnerable populations are also at risk of worsening mental health during extreme heat events (Gong, Part, & Hajat, 2022; Wei et al., 2019; Xu et al., 2019). Because of their relative surface area and rate of metabolism, children are at a higher risk than adults of overheating (Mangus & Canares, 2019). Children and adults can be impacted during outdoor recreation from a lack of tree cover or appropriate shade. In Phoenix, Arizona, extremely high surface temperatures were found on children's recreational playground equipment. Playground steps made out of black powder coated metal were recorded at over 57˚C (136˚F) (Vanos et al., 2016).

The UHIE is impactful for humans during the heat of the day, but the real noticeable difference is felt at night. After the sun has set, impervious surfaces in cities slowly release the heat of the day. As days go by in spring and summer, this lingering heat begins compounding (Sultana & Satyanarayana, 2019). Each day begins at a higher temperature which increases the overall heat in these areas (Veena et al., 2020). Differences in temperature may vary by as much as 12.2˚C (22˚F) and are notably higher when an urban area has less green space and more impervious surfaces. The UHIE is not just compounding over the course of days, each year as ground cover transitions to more impervious surfaces, the intensity of this phenomenon is increasing (Sultana & Satyanarayana, 2020). Further, heat waves can intensify night UHIE, which could be explained by increased surface solar radiation (Jiang et al., 2019). With expected rising urban populations, independent extreme heat events are predicted to increase and become compounded, with the greatest impact being seen in urban areas (Liao et al., 2021; Wang et al., 2021). The period of 2013-2021 was believed to be the warmest decade in history (Lindsey and Dahlman, 2023).

1.2. UHIE and Energy Cost

During dangerously high temperatures, humans rely on air conditioners and electricity-powered fans to keep themselves safe and comfortable. The United States government advises precautions that the strongest protective factor against heat-related illness being air conditioning (National Weather Service,

2022). Urban heat islands increase both overall electricity demand, as well as peak energy demand. Peak demand generally occurs on summer weekdays, late in the afternoons, when offices and homes are running air-conditioning systems, lights, and appliances (Pennsylvania-New Jersey-Maryland Interconnection, 2020). During extreme heat events, which are exacerbated by heat islands, the increased demand for air conditioning can overload systems and require a utility to institute controlled, rolling brownouts to avoid power outages (Auffhammer et al., 2017). The increased energy consumption during extreme heat leads to elevated emissions of air pollutants and greenhouse gases, which contribute to more ground level ozone (Kennedy et al., 2009). This smog is a contributing factor to more UHIE, which feeds into a viscous cycle.

1.3. Trees Equity

The concept of "***tree equity***" in the United States has emerged in the last fifteen years, spotlighting the inequality in vegetation (tree) cover among communities with different level of income and race (Memon et al., 2009). Studies have shown that neighborhoods comprised of minority groups and people of low socioeconomic status disproportionately experience extreme heat, in addition to the corresponding impacts of their quality of life and health (Saverino et al., 2021). People living in socioeconomic disadvantageous conditions (in terms of education and income) are those affected the most by urbanization diseconomies when compared to their counterparts in rural areas (Lenzi and Perucca, 2022). Vulnerability to extreme heat is reduced by higher income and intensified by poverty (Lim and Skidmore, 2020). There are consequences to tree inequity, and one of the most noticeable and measurable phenomena is the direct temperature effects of tree canopy cover. An increase of tree canopy coverage is connected to a lower summer average temperature, which has health implications for those who reside in areas with less tree canopy coverage. An increase in forest coverage has been found to decrease health related mortality and overall community vulnerability to heat effect of climate change (Walton et al. 2016). Children and elderly residents are populations who are more at risk of health complications resulting from extreme high temperatures. In addition, since energy consumption is greater in these areas, those at a lower socioeconomic status feel the economic strain for air conditioning the greatest.

Methods to detect micro-scale heat risk assessment of climatological changes are being developed (Ellena et al., 2023). Studies surrounding anthropogenic climatological changes and their impacts on urban areas have increasingly become the focus of climate research, but there are still limitations with comparisons of socioeconomic and landcover variables between larger cities (Shepherd et al., 2002; Hass et al., 2016; Ellis et al., 2017; Howe et al., 2017; Tirpak et al., 2018; Gichuhi and Gamage, 2023). This study evaluated the urban forest from a spatial perspective. We investigated the variability in mean evapotranspiration in relation to developed land cover and socioeconomic factors. Specifically, by focusing across the major metropolitan areas within Tennessee, we investigate

where do urban heat islands exist and what socioeconomic disparities exist that perpetuate tree inequities? Unlike most UHIE studies, evapotranspiration was the focus of this research, instead of temperature because evapotranspiration is the most significant component of the hydrological budget after precipitation (Hanson, 1991) and the increase of evapotranspiration in cities, using vegetation, urban agriculture, and bodies of water has been accepted as an effective mitigation tool against urban heat islands (Qiu et al., 2013). The purpose of this research was to identify urban heat islands and explore tree equity in Tennessee.

2. Materials and Methods

2.1. Study Area

This study focuses on the area inside the political boundary of twelve urban areas (Table 1) in Tennessee, USA. The term "urban area" is defined as urbanized areas of 50,000 or more humans in the population and urban clusters of at least 2500 but no more than 50,000 humans in the population (United States Bureau of the Census, 2021). Areas are considered rural when they have a population of less than 50,000 humans (Groves, 2011).

Data changes from 2000 to 2010 shown in Table 2 confirm an overall trend of steady growth for all but one reported urban area (United States Bureau of the Census, 2021). Urbanization has impacted land cover in Tennessee. Aside from the majority of land being forested, a large area of West Tennessee is cropland, and Middle and East Tennessee both have areas of pasture and cropland. Overall, clumps of red signify development and increased impervious surface amongst a predominantly forested land cover. Data is examined at the census-tract level and then expanded to county-level.

Table 1. Tennessee urban* areas by population (Tennessee Department of Health, 2022).

Rank	City	County	2015 Estimate
1	Memphis	Shelby	655,780
2	Nashville	Davidson	654,610
3	Knoxville	Knox	185,291
4	Chattanooga	Hamilton	176,588
5	Clarksville	Montgomery	149,176
6	Murfreesboro	Rutherford	126,118
7	Franklin	Williamson	72,639
8	Jackson	Madison	66,975
9	Johnson City	Washington, Carter, Sullivan	66,027
10	Bartlett	Shelby	58,579
11	Hendersonville	Sumner	56,018
12	Kingsport	Sullivan, Hawkins, Washington	53,014

*Note: Defined as urban by having population of 50,000 or more.

Table 2. Tennessee urban area population change from 2000 to 2010 (United States Census, 2010).

Urban Area	2010 population	2000 population	2000-2010 population change	2000-2010 population percentage change
Knoxville, TN	558,696	419,830	138,866	33.08
Clarksville, TN-- KY	158,655	121,775	36,880	30.29
Nashville-Davidson, TN	969,587	749,935	219,652	29.29
Bristol, TN--VA	69,501	58,472	11,029	18.86
Johnson City, TN	120,415	102,456	17,959	17.53
Cleveland, TN	66,777	58,192	8585	14.75
Kingsport, TN	106,571	95,766	10,805	11.28
Chattanooga, TN-- GA	381,112	343,509	37,603	10.95
Jackson, TN	71,880	65,086	6794	10.44
Memphis, TN-- MS--AR	1,060,061	972,091	87,970	9.05
Morristown, TN	59,036	54,368	4668	8.59
Murfreesboro, TN	133,228	135,855	(2627)	−1.93

2.2. Data Acquisition and Manipulation

2.2.1. Population Data

The human data used in this study was median household income and population data at the census tract level, both obtained from the 2020 American Community Survey (ACS) 5-year data set (2018-2022) (ArcGIS, 2022). The U.S. Census defined poverty thresholds in 2021 as annual incomes lower than $13,788 for one person, $17,529 for two people, and $21,559 for three people (United States Bureau of the Census, 2023). Thresholds are defined in increments of one person up to nine people or more in the family. Values vary slightly for the number of children accounted in the household total. The population layer has been symbolized by Environmental Systems Research Institute, Inc. (ESRI) to show the percentage of the population whose income falls below the federal poverty line. For this study, racial diversity data is the percentage of the population that identify as black and having Hispanic background. Boundaries in this data set come from the US Census TIGER geodatabases.

2.2.2. Land Cover Data

Land cover data was obtained from the National Land Cover Database (NLCD), supplied through ESRI Living Atlas (MRLC, 2022). NLCD produces products through the Multi-Resolution Land Characteristics (MRLC) Consortium. The MRLC Consortium is a large partnership of federal agencies including the U.S. Geological Survey, the National Oceanic and Atmospheric Administration, the U.S. Environmental Protection Agency, the U.S. Department of Agriculture, the U.S. Forest Service, the National Park Service, the U.S. Fish and Wildlife Service, the Bureau of Land Management and the USDA Natural Resources Conserva-

tion Service. Although it is described as having information "to present", the most recent data available is 2019. Unsigned Char is the pixel type utilized. The cell size is 30/30 meter. The spatial reference information for the NLCD is North America Albers projection. Developed land cover percentage and forest land cover percentage were the land cover classes used for this study.

2.2.3. Road Density Data

Road density data was obtained from ESRI. An inverse of this variable was used to reflect the greater coverage of impervious surface cover from roadways. Spatial and temporal characteristics of road networks and correlations with urban expansion are used for optimization of development (Zhao et al., 2017). Road density should also be considered for its impact on microclimate.

2.2.4. Evapotranspiration Data

Data showing mean evapotranspiration levels were obtained from the Operational Simplified Energy Balance (SSEBop) (Senay et al., 2020). SSEBop is a remote-sensing based model that provides actual evapotranspiration estimates using the SSEBop model and evapotranspiration fractions from the National Atmospheric Space Administration's Moderate Resolution Imaging Spectroradiometer and predefined parameters for operational applications. This live feed is automatically updated monthly. Mean evapotranspiration units are reported in millimeters per month. Cell size is .01 degrees (~1 km). The source type is stretched. The pixel type is 16 Bit Integer. The data and mosaic projections are both Geographic Coordinate System World Geodetic System 1984 (GCS WGS84) with global extent. The source is United States Geological Survey Famine Early Warning Systems Network (USGS – FEWS Net) Monthly Actual Evapotranspiration (ET).

2.3. Data Analysis

Data analysis was a multi-step process which included choosing variables, examining the distribution of data variables, examining the data for global trends and patterns, examining local variation and examining the spatial autocorrelation and testing hypotheses. Map layers containing data from ACS, NLCD, and SSEBop were added to a map in ArcGIS Online (hereafter AGOL). The base map was enriched with evapotranspiration, land cover (forest and developed), and average household income data. A spatial analysis was performed to display the relationship of the percent of forested land cover and the percent of developed land cover. The mean evapotranspiration map was created to display mean evapotranspiration levels across the state as a comparison of the impact of land cover type on evapotranspiration, with areas of most evapotranspiration being dark blue and going lighter as the evapotranspiration level approaches zero (**Map 1**).

A ratio of evapotranspiration and landcover was calculated to display and calculate hot/cold spot areas with evapotranspiration compared with landcover.

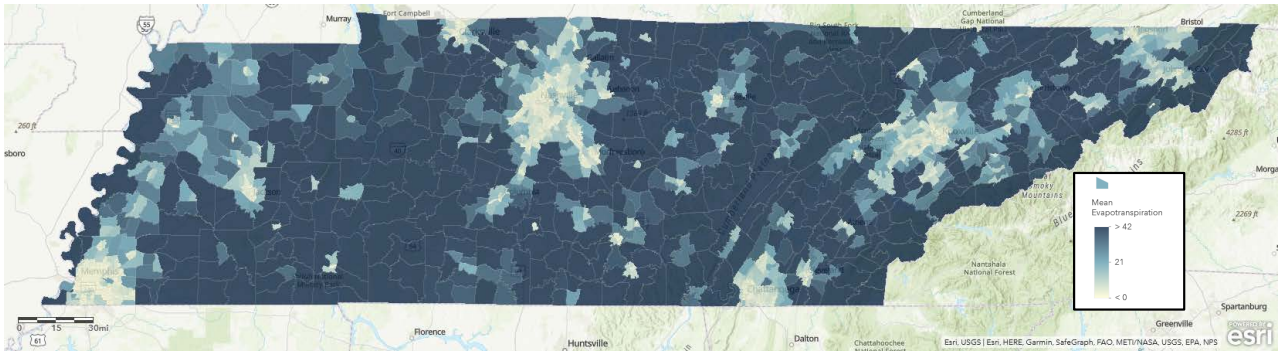

Map 1. Variability of evapotranspiration levels (in mm) across Tennessee.

The Hot Spot Analysis Tool identified statistically significant spatial clusters of high and low values of the ratio of evapotranspiration and developed land cover. Using the Hot Spot tool, the Getis-Ord Gi statistic was calculated for each feature in the dataset with corresponding z-scores and p values. The tool calculated optimal defaults and automatically applied a false discovery rate correction. A GIS-based multivariate spatial clustering approach was also used to identify where different levels of evapotranspiration grouped with income, percent developed land, income, air conditioner ownership and population density. A total of three optimal clusters were computed and displayed based on the pseudo f score that was calculated from the machine learning clustering algorithm.

An overall model to predict mean evapotranspiration was hypothesized and constructed using Ordinary Least Squares regression. Initially, all variables were examined in an exploratory regression model to determine which variables had the most impact on mean evapotranspiration without violating assumptions of multiple regression including VIF values. The model with the variables that had the most explanatory value, or the highest R2 and lowest AICc, without violating assumptions of multiple regression, was chosen to predict mean evapotranspiration. The variables chosen to predict mean evapotranspiration were then modeled in OLS and generalized linear regression models and subsequently a geographically weighted regression model. The model was tested for spatial autocorrelation before constructing a spatially autocorrelated regression model. Spatial autocorrelation identifies the correlation of a variable with itself across space. If positive spatial autocorrelation exists, units that are close to each other are more likely to be similar to each other. Therefore the residuals are not independent, which is one key component of OLS regression. In the absence of spatial autocorrelation, OLS linear regression can be used to predict a dependent variable from independent variables.

An OLS model was constructed to predict mean evapotranspiration. Independent variables hypothesized to predict mean evapotranspiration included the census variables of Median household income defined by the ACS survey, percent of land developed, percent of land designated as forest, road density, population density, the percent of households that owned an air conditioner. The overall OLS model was significant, where calculation F (x, y) = Z, $p < .05$. But

positive spatial autocorrelation was also significant. Global Moran's I was used to test spatial autocorrelation in residuals of regression. Global Moran's I tests whether the geospatial pattern of variables is spatially clustered. Global Moran's I calculates an index score alongside a z-score and p-value to evaluate the significance. Multiple iterations of Global Moran's I were calculated using census tract values variables. Spatial clustering was significant within census tracts using both inverse distance weights and K-nearest neighbor weights up to 1000 neighbors. The presence of spatial clustering can increase the likelihood of Type 1 errors in statistical analyses if the spatial dependencies are not properly accounted for or adjusted in the analysis. A type 1 error occurs when a statistical model falsely identifies a relationship or significance that does not actually exist. Generally, it is a false positive outcome where the model erroneously indicates that certain variables are influencing an outcome when they are not. To mitigate the risk of Type 1 errors in our analysis, we decided to aggregate the values to the county level and conducted multiple iterations of spatial autocorrelation testing to ensure the robustness of our findings. Spatial autocorrelation was no longer significant when K-nearest neighbors spatial weights matrix was used and the minimum value for nearest neighbors was set to 8. The lowest AIC and highest R2 occurred with county level data when spatial weights matrix of 35 neighbors was used. This resulted in a predictive R2 value of .822 and an AIC of 660.11.

The initial OLS model predicted evapotranspiration at the county level using the following independent variables; 1) population density, 2) median household income, 3) road density, 4) residents with central air conditioning, 5) developed land cover, and 6) forested land cover, with a geographically weighted regression model. The model was again tested for spatial autocorrelation. Spatial weights were constructed using K-nearest neighbors and inverse distance bands. In the residuals of the final full model Moran's I was not significant when the neighborhood size was conceptualized using a spatial weights matrix with a maximum inverse distance of 46,920 meters (z = 1.7, p = .08) and with a spatial weights matrix of at least 8 neighbors in a K-nearest neighbors configuration. (z = .52, p = .601). With spatial autocorrelation considered, a geographically weighted regression model (Spatial autoregressive model) was then used to predict evapotranspiration within counties.

3. Results

Model Diagnostics using spatial weights of k nearest neighbors were run in multiple iterations with of K = 35 neighbors, being the model that best accounted for spatial autocorrelation. The results were significant with R2 equaling .8222, AdjR2 equaling .7815, and AICc equaling 660.1063

3.1. Mean Evapotranspiration Levels and the Relationship Between Develop and Forest Cover

We obtained 1701 actual evapotranspiration estimates using the SSEBop model

and evapotranspiration fractions from the National Atmospheric Space Administration's Moderate Resolution Imaging Spectroradiometer. The minimum mean evapotranspiration level was 0 millimeters per month (mm/month) and the maximum of 97.1 mm/month. Lower evapotranspiration rates are lighter in color (white) whereas the higher the evapotranspiration rate the darker the color (blue) Map 1. The average mean evapotranspiration level across the state of TN is 20.92 mm/month. Most areas with forest cover and bodies of water have mean evapotranspiration levels greater than 30 millimeters per month, which creates a dark blue backdrop for the state (Map 1). On average, across Tennessee monthly, the nine major metropolitan areas with the highest populations have the low evapotranspiration levels (Table 1).

Tennessee is a forested state with large areas across the state with low levels of development (Map 2). We categorize forested land cover as "low" (>23%), a mid-range between 23% and 43% and "high" with greater than 43%. We categorize developed land cover as "low" (>11%), a mid-range between 11% and 35% and "high" with greater than 35%. Lastly, agricultural land (crops and pasture) designation is maroon and represents low levels of vegetation and low levels of impervious surface cover. Forest cover across the state ranges from 2.5% to 94.8%, with an average forest cover of 34.8%. In contrast, urban areas that have significant development on Map 2 (designated as purple), meaning these areas have relatively low levels of vegetation and high levels of impervious surface cover. Development (built environment) ranges were observed from 1.2% to 94.8%, with an average of 31.41%.

Evapotranspiration is categorized as "low" with less than 5 mm/month, a mid-range with more than 5 mm/month and less than 24 mm/month, and "high" with greater than 24 mm/month. Map 3 highlights the relationship between mean evapotranspiration levels and developed land cover, where bold orange symbolized the top seven urban ranked areas from Table 1, with high levels of developed land cover and low levels of evapotranspiration. These urban areas specifically have the least evapotranspiration when compared to less developed, more forested land cover. Two outliers exist where there is high evapotranspiration and high developed land cover. The cities of Crossville and Cleveland are located near large bodies of water, Lake Holiday and the Hiwassee River, respectively. We hypothesize that, due to these two large bodies' proximity to developed areas, evapotranspiration levels remain relatively high.

3.2. Mean Evapotranspiration Levels, Developed Land Cover, Hot Spot Analysis and Households

Since there was significant spatial clustering at the tract level, a hot spot analysis was conducted. A hot spot analysis uses the Gettis-Ord Gi to measure local indicators of spatial association by identifying spatial clusters of high values (hot spots) or low values (cold spots) of evapotranspiration We conducted Hot Spot Analysis to determine areas across the state that had the lowest mean evapotranspiration level in relation to the highest developed land cover. The city of

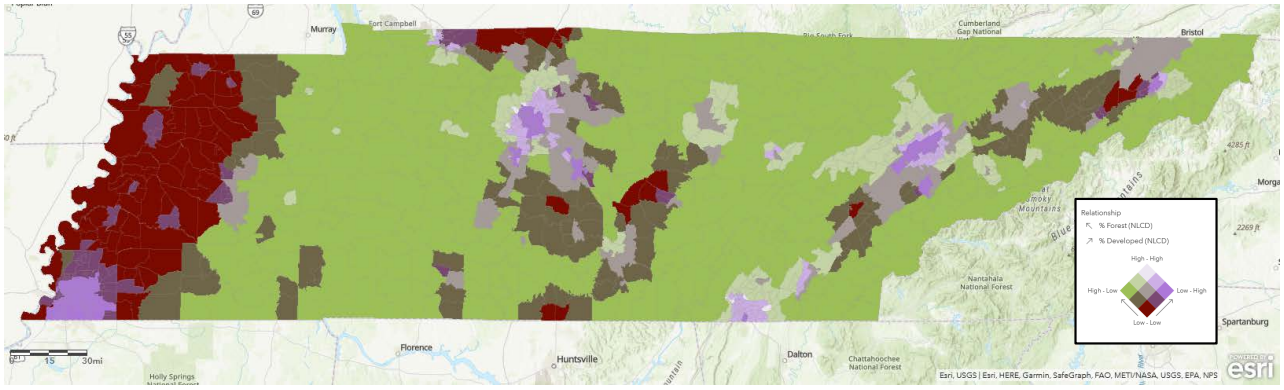

Map 2. Relationship between forested and developed land cover in Tennessee.

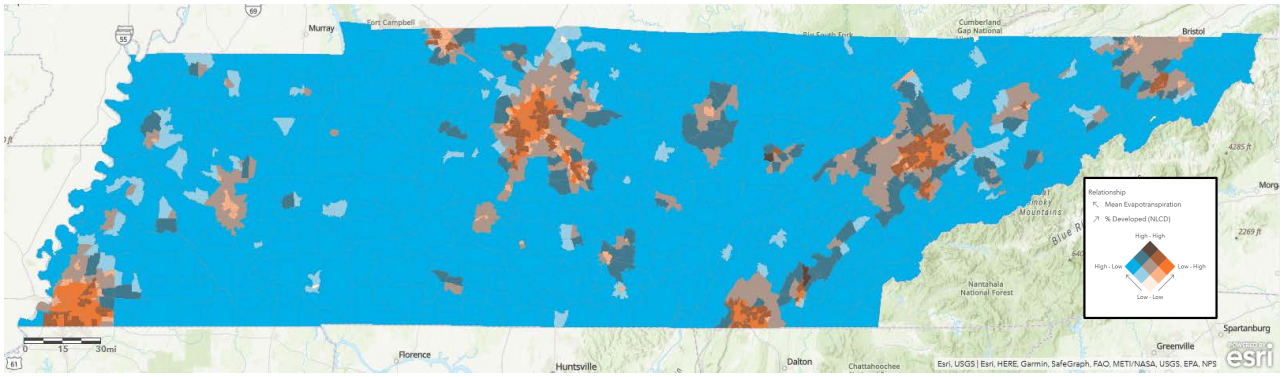

Map 3. Relationship between evapotranspiration and developed land cover in TN.

Memphis, located in the southwest corner of the state, showed a Hot Spot with 99% confidence (Map 4). The largest hot spot area is Nashville, extending past Nashville proper to surrounding communities like Franklin to the southwest, Murfreesboro to the southeast, and Gallatin to the northeast. Due east, Knoxville and surrounding areas like Oak Ridge to the northwest create a hot spot rivaling Nashville. In southeast Tennessee, Chattanooga has a hot spot with half the area in the 99% confidence level. A small hot spot with 95% confidence is over Kingsport in northeast Tennessee. The relationship between mean evapotranspiration and 2020 households with income below poverty level appeared to have more random distribution of high and low levels of the variables across the state. Evaporation is categorized as "low" with less than 5 mm/month, a mid-range with more than 5 mm/month and less than 24 mm/month, and "high" with greater than 24 mm/month. Hot Spot analysis with mean evapotranspiration levels and rate of poverty created five hot spots with at least 95% confidence, Memphis > Nashville > Knoxville > Chattanooga and Tri-Cities.

3.3. Tract-Level Generalized Linear Regression Model and Multivariate Clustering Analysis

The generalized linear regression model with tract-level (or OLS) was developed using median household income, developed land cover, forested land cover,

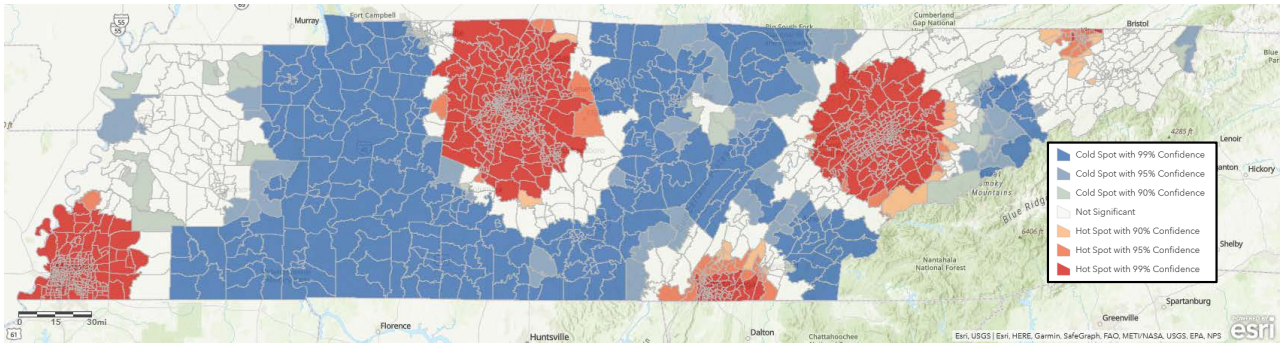

Map 4. Hot spot analysis with evapotranspiration and developed land cover in TN.

households with an air conditioner, road density and population density. This model showed statistical significance with an adjusted R^2 value of .55 F (6, 1694) = 349.14. Spatial clustering and spatial autocorrelation were indicated by significance of the Koenker (BP) Statistic (370.718). In addition, the Jarque Bera Statistic was also significant (125.196), which indicates that the residuals are not normally distributed. Global Moran's I result were significant, showing significant spatial clustering at multiple distances. Since the results indicated that there was significant spatial clustering, multivariate clustering method was used.

Multivariate clustering was employed to further explore the data at the tract level. The multivariate clustering tool utilizes unsupervised machine learning to find natural clusters of census tract values. This classification method is considered an unsupervised machine learning method because it did not require training data to find clusters. The tool evaluated the optimal number of clusters by computing a pseudo F-statistic for 2 - 30 clusters. The highest pseudo F statistic represents the optimal number of clusters that maximizes within-cluster similarities and between-cluster differences. in this case, the pseudo F statistic indicated that three clusters was most effective at describing the clusters within the data. The variable distribution to the k-means clustering ranged from R^2 values between .59 and .41 for census tracts. The first cluster had 744 census tracts, the second cluster had 437 census blocks and the third cluster had 520 blocks (**Table 3**). Areas in blue represent the highest mean evapotranspiration levels, the lowest percentage of developed land, a relatively low level of median household income, a mid-level of households with central air conditioner, and the lowest level of population density (**Map 5**, **Table 3**). Areas in red represent the highest level of median household income, the greatest number of households with central air conditioner, a mid-level of developed land cover, low evapotranspiration, a mid-level of population density. Areas in green are considered the communities that are most vulnerable to urban heat island effects and represent the lowest median household income, the highest level of developed land, the lowest evapotranspiration levels, the lowest percentage of households with central air conditioner, and the highest population density.

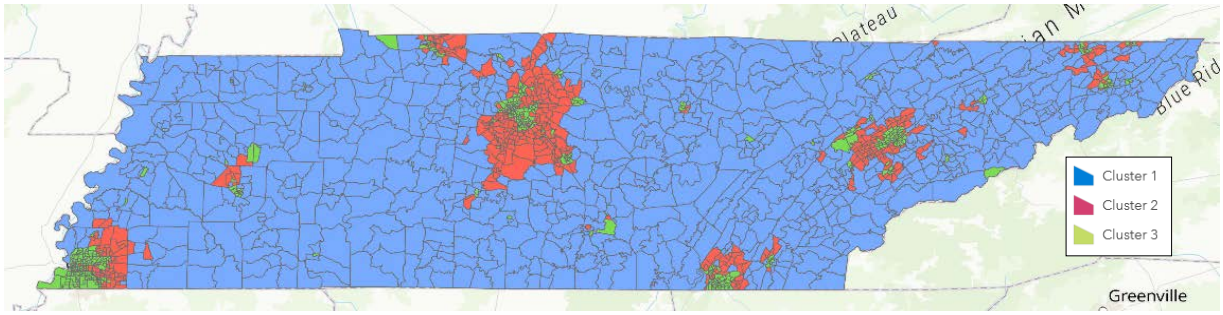

Map 5. Multivariate cluster analysis with household income, developed land cover, evapotranspiration levels, households with central air and population density.

Table 3. Cluster group analysis results.

Cluster ID (Group By)	Alias	Mean	Standard Deviation	Median	Count	Coefficient of Variation
1	2020 Median HH Income (ACS 5-Yr)	$49365.6	12136.14	48001	744	0.25
1	% Developed (NLCD)	9.6	6.05	7.6	744	0.63
1	Mean Evapotranspiration (in mm)	39.2	19.59	38.3	744	0.50
1	2022 HH Has Central Air Conditioner: Percent	44.8	5.33	45.07	744	0.12
1	2020 Population Density	192.6	250.70	99.5	744	1.30
2	2020 Median HH Income (ACS 5-Yr)	$88692.1	30987.00	79948	437	0.35
2	% Developed (NLCD)	35.3	19.86	29.7	437	0.56
2	Mean Evapotranspiration (in mm)	9.7	7.88	7.4	437	0.81
2	2022 HH Has Central Air Conditioner: Percent	53.1	5.25	54.11	437	0.10
2	2020 Population Density	1389.2	1048.73	1121.5	437	0.75
3	2020 Median HH Income (ACS 5-Yr)	$40191.8	17544.00	39483	520	0.44
3	% Developed (NLCD)	59.3	25.25	62.7	520	0.43
3	Mean Evapotranspiration (in mm)	4.1	5.20	2.5	520	1.25
3	2022 HH Has Central Air Conditioner: Percent	33.6	9.10	35.06	520	0.27
3	2020 Population Density	3099.6	2439.89	2701.4	520	0.79

4. Discussion

The ordinary least squares regression model shows statistical significance for predicting mean evapotranspiration at the county level using population density, residents with central air conditioning, forested land cover, developed land cover, median household income, and road density. Meta-analysis has revealed significant income-based inequity in urban forests and highlights the impact of accounting for spatial autocorrelation (Gerrish and Watkins, 2018). Poisson regression has previously shown that forest characteristics, age, race and urbanicity have a significant influence on county heat mortality (Walton et al., 2016). Further, a Poisson regression model on using Memphis data from 2008-2017 found higher cardiovascular mortality risk in heatwave days where the maxi-

mum daily temperature is greater than the 95th percentile for more than two consecutive days (Li et al., 2019). Their results indicated that socioeconomic status, race and urbanicity did not impact the mortality rate. In contrast, heat illness data from Florida shows that high income counties consistently have lower health risks of dehydration, heat-related illness, acute renal disease, and respiratory disease, and socioeconomic demographic variables were significantly associated with the magnitude of heat-related health risks (Jung et al., 2021).

Increased tree canopy coverage in urban areas of Tennessee is necessary to mitigate urban heat island effects, including decreased mean evapotranspiration. Active urban forest management with focuses on responsible urban growth, land use planning, and urban forest cultivation should be the goals of all urban areas in Tennessee for improved climate stability and community health. Municipalities should be encouraged to create Tree Boards whose purpose includes monitoring tree canopy, ensuring tree equity across all socioeconomic communities, proposing legislation protecting native trees when necessary and holding land developers accountable for responsible natural resources management. Municipalities should also have a professional or team of professionals focusing on urban green space planning. Green spaces containing predominantly vegetation can significantly reduce land surface temperature in urban areas that surround them (Yao et al., 2022; Loughner et al., 2012).

Green infrastructure development investment will benefit disadvantaged residents in low-income areas who currently disproportionately feel the effects of urban heat islands. Tennessee's most vulnerable communities are the areas with the highest need for UHIE mitigation assistance. A group of Census tracts were identified as vulnerable communities and should be the focus of tree equitability remediations. Tree equity can come into balance through the municipal implementation of green infrastructure. Future directions of research and policy development should consider focusing on historically low-income urban areas and underserved communities. Municipal occupation records can be evaluated for structures that are chronically unused or unusable. Planning grants can be offered to property owners who have strategies to take their unused structure and make it of use through occupation or destruction and conversion to a different, functional land cover. An evaluative instrument could be created to give buildings a score for their communal and environmental function. A minimum threshold can be determined for further investigation into properties. Impervious surfaces create an increased need for anthropogenic energy use to keep humans and their things comfortable and safe from extreme heat. This costs money and adds emissions that further fuel UHIE. Urban forests should be planned with surrounding building height, tree location, and vertical leaf area in mind (Yun et al., 2020). For shade cooling of common urban surfaces, surface material surrounding trees created a greater impact than tree species (Kaluarachichi et al., 2020). Mature trees are better than younger saplings; when evaluating climate regulating ecosystem services, trunk circumference has been found to be a valu-

able indicator for estimation (Helletsgruber et al., 2020).

Implementation and planning funding, lack of community and nongovernmental organizational support, development pressure in urban and greenfield areas, and law and policy establishment are among the biggest urban forest governance challenges (Wirtz et al., 2021). It is important to learn residents' perspectives, interests, and desires for the urban forest, since community involvement bolsters the chances of successful urban forest management (Van Herzele et al., 2005; Sheppard et al., 2017; Tran et al., 2017; Butt et al., 2021). Collaborative efforts should be pursued by government agencies in partnership with community members who will ultimately interact with the urban forests and benefits they provide.

5. Conclusion

This work provides an overview of geospatial methods for UHIE assessment. The most urbanized areas that are farther from forest land cover, with the greatest amount of impervious cover and road density are most impacted by urban heat island effects. Among these inner-city areas are vulnerable communities, predominantly inhabited by higher rates of the population with the lowest median household income levels in Tennessee, who also have the least number of central air conditioners in their households, meaning people with fewer financial resources are most susceptible to harmful urban heat island effects. These findings demonstrate that in addition to UHIE mitigation efforts, considerations should be made for vulnerable communities of resource allocation and collaborative management (residents and municipalities) of urban forests. Evapotranspiration levels can be predicted by changing variables of forested land cover, developed land cover, road density, and population density, giving policy makers and land use planners the ability to estimate expected climatological changes from anthropogenic impacts.

Conflicts of Interest

The authors declare no conflicts of interest regarding the publication of this paper.

References

ArcGIS (2022). *U.S. Census Bureau's American Community Survey (ACS) 2017-2021 5-Year Estimates*. Table(s) B17020, C17002. https://services.arcgis.com/P3ePLMYs2RVChkJx/arcgis/rest/services/ACS_Poverty_by_Age_Centroids/FeatureServer

Auffhammer, M., Baylis, P., & Hausman, C. (2017). Climate Change Is Projected to Have Severe Impacts on the Frequency and Intensity of Peak Electricity Demand across the United States. *Proceedings of the National Academy of Sciences of the United States of America, 114,* 1886-1891. https://doi.org/10.1073/pnas.1613193114

Butt, S., Smith, S. M., Moola, F., & Conway, T. M. (2021). The Relationship between Knowledge and Community Engagement in Local Urban Forest Governance: A Case

Study Examining the Role of Resident Association Members in Mississauga, Canada. *Urban Forestry & Urban Greening, 60,* Article 127054. https://doi.org/10.1016/j.ufug.2021.127054

Ellena, M., Melis, G., Zengarini, N., Di Gangi, E., Ricciardi, G. K., Mercogliano, P., & Costa, G. (2023). Micro-Scale UHI Risk Assessment on the Heat-Health Nexus within Cities by Looking at Socio-Economic Factors and Built Environment Characteristics: The Turin Case Study (Italy). *Urban Climate, 49,* Article 101514. https://doi.org/10.1016/j.uclim.2023.101514

Ellis, K. N., Hathaway, J. M., Mason, L. R., Howe, D. A., Epps, T. H., & Brown, V. M. (2017). Summer Temperature Variability across Four Urban Neighborhoods in Knoxville, Tennessee, USA. *Theoretical and Applied Climatology, 127,* 701-710. https://doi.org/10.1007/s00704-015-1659-8

Gartland, L. M. (2012). *Heat Islands: Understanding and Mitigating Heat in Urban Areas*. Routledge. https://books.google.com/books?id=O53hhhSJFc4C&printsec=frontcover&source=gbs_ge_summary_r&cad=0#v=onepage&q&f=false https://doi.org/10.4324/9781849771559

Gerrish, E., & Watkins, S. L. (2018). The Relationship between Urban Forests and Income: A Meta-Analysis. *Landscape and Urban Planning, 170,* 293-308. https://doi.org/10.1016/j.landurbplan.2017.09.005

Gichuhi, W. K., & Gamage, L. (2023). Efficacy of the CO Tracer Technique in Partitioning Biogenic and Anthropogenic Atmospheric CO_2 Signals in the Humid Subtropical Eastern Highland Rim City of Cookeville, Tennessee. *Atmosphere, 14,* Article 208. https://doi.org/10.3390/atmos14020208

Gong, J., Part, C., & Hajat, S. (2022). Current and Future Burdens of Heat-Related Dementia Hospital Admissions in England. *Environment International, 159,* Article 107027. https://doi.org/10.1016/j.envint.2021.107027

Groves, R. M. (2011). *Urban Area Criteria for the 2010 Census*. https://www.federalregister.gov/documents/2011/08/24/2011-21647/urban-area-criteria-for-the-2010-census

Hanson, R. (1991). *Evapotranspiration and Droughts*. https://geochange.er.usgs.gov/sw/changes/natural/et/

Hass, A. L., Ellis, K. N., Mason, L. R., Hathaway, J. M., & Howe, D. A. (2016). Heat and Humidity in the City: Neighborhood Heat Index Variability in a Mid-Sized City in the Southeastern United States. *International Journal of Environmental Research and Public Health, 13,* Article 117. https://doi.org/10.3390/ijerph13010117

Helletsgruber, C., Gillner, S., Gulyás, Á., Junker, R. R., Tanács, E., & Hof, A. (2020). Identifying Tree Traits for Cooling Urban Heat Islands—A Cross-City Empirical Analysis. *Forests, 11,* Article 1064. https://doi.org/10.3390/f11101064

Howe, D. A., Hathaway, J. M., Ellis, K. N., & Mason, L. R. (2017). Spatial and Temporal Variability of Air Temperature across Urban Neighborhoods with Varying Amounts of Tree Canopy. *Urban Forestry & Urban Greening, 27,* 109-116. https://doi.org/10.1016/j.ufug.2017.07.001

Iungman, T., Cirach, M., Marando, F., Barboza, E. P., Khomenko, S., Masselot, P. et al. (2023). Cooling Cities through Urban Green Infrastructure: A Health Impact Assessment of European Cities. *The Lancet, 401,* 577-589. https://doi.org/10.1016/S0140-6736(22)02585-5

Jiang, S., Lee, X., Wang, J., & Wang, K. (2019). Amplified Urban Heat Islands during Heat Wave Periods. *Journal of Geophysical Research: Atmospheres, 124,* 7797-7812.

https://doi.org/10.1029/2018JD030230

Jung, J., Uejio, C. K., Kintziger, K. W., DuClos, C., Reid, K., Jordan, M., & Spector, J. T. (2021). Heat Illness Data Strengthens Vulnerability Maps. *BMC Public Health, 21,* Article No. 1999. https://doi.org/10.1186/s12889-021-12097-6

Kaluarachichi, T. U. N., Tjoelker, M. G., & Pfautsch, S. (2020). Temperature Reduction in Urban Surface Materials through Tree Shading Depends on Surface Type Not Tree Species. *Forests, 11,* Article 1141. https://doi.org/10.3390/f11111141

Kennedy, C., Steinberger, J., Gasson, B., Hansen, Y., Hillman, T., Havranek, M. et al. (2009). Greenhouse Gas Emissions from Global Cities. *Environmental Science & Technology, 43,* 7297-7302. https://doi.org/10.1021/es900213p

Lenzi, C., & Perucca, G. (2022). No Place for Poor Men: On the Asymmetric Effect of Urbanization on Life Satisfaction. *Social Indicators Research, 164,* 165-187. https://doi.org/10.1007/s11205-022-02946-1

Li, Y., Akkus, C., Yu, X., Joyner, T. A., Kmet, J., Sweat, D., & Jia, C. (2019). Heatwave Events and Mortality Outcomes in Memphis, Tennessee: Testing Effect Modification by Socioeconomic Status and Urbanicity. *International Journal of Environmental Research and Public Health, 16,* Article 4568. https://doi.org/10.3390/ijerph16224568

Liao, W., Li, D., Malyshev, S., Shevliakova, E., Zhang, H., & Liu, X. (2021). Amplified Increases of Compound Hot Extremes over Urban Land in China. *Geophysical Research Letters, 48,* e2020GL091252. https://doi.org/10.1029/2020GL091252

Lim, J., & Skidmore, M. (2020). Heat Vulnerability and Heat Island Mitigation in the United States. *Atmosphere, 11,* Article 558. https://doi.org/10.3390/atmos11060558

Lindsey, R., & Dahlman, L. (2023). *Climate Change: Global Temperature*. https://www.climate.gov/news-features/understanding-climate/climate-change-global-temperature

Loughner, C. P., Allen, D. J., Zhang, D., Pickering, K., Dickerson, R. R., & Landry, L. A. (2012). Roles of Urban Tree Canopy and Buildings in Urban Heat Island Effects: Parameterization and Preliminary Results. *Journal of Applied Meteorology and Climatology, 51,* 1775-1793. https://doi.org/10.1175/JAMC-D-11-0228.1

Mangus, C. W., & Canares, T. (2019). Heat-Related Illness in Children in an Era of Extreme Temperatures. *Pediatrics in Review, 40,* 97-107. https://doi.org/10.1542/pir.2017-0322

Memon, R. A., Leung, D. Y., & Liu, C. (2009). An Investigation of Urban Heat Island Intensity (UHII) as an Indicator of Urban Heating. *Atmospheric Research, 94,* 491-500. https://doi.org/10.1016/j.atmosres.2009.07.006

Multi-Resolution Land Characteristics (MRLC) Consortium. National Land Cover Data. https://landscape10.arcgis.com/arcgis/rest/services/USA_NLCD_Land_Cover/ImageServer

National Weather Service (2022). *Heat Safety: U.S. National Oceanic and Atmospheric Administration*. https://www.weather.gov/grb/heat

Pennsylvania-New Jersey-Maryland Interconnection (PJM) (2020). *How Energy Use Varies with the Seasons: Pennsylvania-New Jersey-Maryland Interconnection*. https://learn.pjm.com/three-priorities/keeping-the-lights-on/how-energy-use-varies

Qiu, G., Li, H., Zhang, Q., Chen, W., Liang, X., & Li, X. (2013). Effects of Evapotranspiration on Mitigation of Urban Temperature by Vegetation and Urban Agriculture. *Journal of Integrative Agriculture, 12,* 1307-1315. https://doi.org/10.1016/S2095-3119(13)60543-2

Saverino, K. C., Routman, E., Lookingbill, T. R., Eanes, A. M., Hoffman, J. S., & Bao, R.

(2021). Thermal Inequity in Richmond, VA: The Effect of an Unjust Evolution of the Urban Landscape on Urban Heat Islands. *Sustainability, 13,* Article 1511. https://doi.org/10.3390/su13031511

Senay, G. B., Kagone, S., & Velpuri, N. M. (2020). Operational Global Actual Evapotranspiration: Development, Evaluation, and Dissemination. *Sensors, 20,* Article 1915. https://doi.org/10.3390/s20071915

Shepherd, J. M., Pierce, H., & Negri, A. J. (2002). Rainfall Modification by Major Urban Areas: Observations from Spaceborne Rain Radar on the TRMM Satellite. *Journal of Applied Meteorology and Climatology, 41,* 689-701. https://doi.org/10.1175/1520-0450(2002)041<0689:RMBMUA>2.0.CO;2

Sheppard, J., Ryan, C. R., & Blahna, D. J. (2017). Evaluating Ecological Monitoring of Civic Environmental Stewardship in the Green-Duwamish Watershed, Washington. *Landscape and Urban Planning, 158,* 87-95. https://doi.org/10.1016/j.landurbplan.2016.09.017

Sultana, S., & Satyanarayana, A. N. V. (2019). Impact of Urbanisation on Urban Heat Island Intensity during Summer and Winter over Indian Metropolitan Cities. *Environmental Monitoring and Assessment, 191,* Article No. 789. https://doi.org/10.1007/s10661-019-7692-9

Sultana, S., & Satyanarayana, A. N. V. (2020). Assessment of Urbanisation and Urban Heat Island Intensities Using Landsat Imageries during 2000-2018 over a Sub-Tropical Indian City. *Sustainable Cities and Society, 52,* Article 101846. https://doi.org/10.1016/j.scs.2019.101846

Tirpak, R. A., Hathaway, J. M., Franklin, J. A., & Khojandi, A. (2018). The Health of Trees in Bioretention: A Survey and Analysis of Influential Variables. *Journal of Sustainable Water in the Built Environment, 4.* https://doi.org/10.1061/JSWBAY.0000865

Tran, Y. L., Siry, J. P., Bowker, J., & Poudyal, N. C. (2017). Atlanta Households' Willingness to Increase Urban Forests to Mitigate Climate Change. *Urban Forestry & Urban Greening, 22,* 84-92. https://doi.org/10.1016/j.ufug.2017.02.003

United States Bureau of the Census (2021). *2010 Census Urban and Rural Classification and Urban Area Criteria.* United States Bureau of Census. https://www.census.gov/programs-surveys/geography/guidance/geo-areas/urban-rural/2010-urban-rural.html

United States Bureau of the Census (2023). *Poverty Thresholds*. United States Bureau of Census. https://www.census.gov/data/tables/time-series/demo/income-poverty/historical-poverty-thresholds.html

Van Herzele, A., De Clercq, E. M., & Wiedemann, T. (2005). Strategic Planning for New Woodlands in the Urban Periphery: Through the Lens of Social Inclusiveness. *Urban Forestry & Urban Greening, 3,* 177-188. https://doi.org/10.1016/j.ufug.2005.01.002

Vanos, J., Middel, A., McKercher, G. R., Kuras, E. R., & Ruddell, B. L. (2016). Hot Playgrounds and Children's Health: A Multiscale Analysis of Surface Temperatures in Arizona, USA. *Landscape and Urban Planning, 146,* 29-42. https://doi.org/10.1016/j.landurbplan.2015.10.007

Veena, K., Parammasivam, K. M., & Venkatesh, T. (2020). Urban Heat Island Studies: Current Status in India and a Comparison with the International Studies. *Journal of Earth System Science, 129,* Article No. 85. https://doi.org/10.1007/s12040-020-1351-y

Walton, Z., Poudyal, N. C., Hepinstall, J. A., Gaither, C. J., & Boley, B. B. (2016). Exploring the Role of Forest Resources in Reducing Community Vulnerability to the Heat Effects of Climate Change. *Forest Policy and Economics, 71,* 94-102.

https://doi.org/10.1016/j.forpol.2015.09.001

Wang, J., Chen, Y., Liao, W., He, G., Tett, S. F. B., Zeng, Y. et al. (2021). Anthropogenic Emissions and Urbanization Increase Risk of Compound Hot Extremes in Cities. *Nature Climate Change, 11,* 1084-1089. https://doi.org/10.1038/s41558-021-01196-2

Wei, Y., Wang, Y., Lin, C., Yin, K., Yang, J., Shi, L. et al. (2019). Associations between Seasonal Temperature and Dementia-Associated Hospitalizations in New England. *Environment International, 126,* 228-233. https://doi.org/10.1016/j.envint.2018.12.054

Wirtz, Z., Hagerman, S., Hauer, R. J., & Konijnendijk, C. C. (2021). What Makes Urban Forest Governance Successful?—A Study among Canadian Experts. *Urban Forestry & Urban Greening, 58,* Article 126901. https://doi.org/10.1016/j.ufug.2020.126901

Xu, Z., Tong, S., Cheng, J., Zhang, Y., Wang, N., Zhang, Y. et al. (2019). Heatwaves, Hospitalizations for Alzheimer's Disease, and Postdischarge Deaths: A Population-Based Cohort Study. *Environmental Research, 178,* Article 108714. https://doi.org/10.1016/j.envres.2019.108714

Yao, X., Yu, K., Zeng, X., Lin, Y., Ye, B., Shen, X., & Liu, J. (2022). How Can Urban Parks Be Planned to Mitigate Urban Heat Island Effect in "Furnace Cities"? An Accumulation Perspective. *Journal of Cleaner Production, 330,* Article 129852. https://doi.org/10.1016/j.jclepro.2021.129852

Yun, S., Park, C. Y., Kim, E. S., & Lee, D. (2020). A Multi-Layer Model for Transpiration of Urban Trees Considering Vertical Structure. *Forests, 11,* Article 1164. https://doi.org/10.3390/f11111164

Zhao, G., Zheng, X., Yuan, Z., & Zhang, L. (2017). Spatial and Temporal Characteristics of Road Networks and Urban Expansion. *Land, 6,* Article 30. https://doi.org/10.3390/land6020030